Multiferroism in hexagonally stabilized $TmFeO_3$ thin films below 120 K

Journal:	*Journal of Materials Chemistry C*
Manuscript ID:	TC-COM-03-2014-000461.R1
Article Type:	Communication
Date Submitted by the Author:	28-Mar-2014
Complete List of Authors:	Ahn, Suk-Jin; Pohang University of Science and Technology (POSTECH), Materials Science and Engineering; Samsung Electronics Co., Memory Manufacturing Operation Center Lee, Jung-Hoon; Pohang University of Science and Technology (POSTECH), Department of Materials Science and Engineering, and Division of Advanced Materials Science Jeong, Youngkyu; Northwestern University, Materials Science and Engineering; Samsung Electronics Co.,

Journal Name RSCPublishing

COMMUNICATION

Multiferroism in hexagonally stabilized $TmFeO_3$ thin films below 120 K

Cite this: DOI: 10.1039/x0xx00000x

Suk-Jin Ahn,[a,c] Jung-Hoon Lee[a] and Young Kyu Jeong[b,c,*]

Received 00th January 2012,
Accepted 00th January 2012

DOI: 10.1039/x0xx00000x

www.rsc.org/

$TmFeO_3$ is known to have an orthorhombic structure characterized by the corner-linked FeO_6 octahedra in a three-dimensional network (space group Pnma). Thus, it is expected to be non-ferroelectric. In the present study, however, we have stabilized a hexagonal $TmFeO_3$ thin-film heterostructure by adopting hexagonal templates. In this way, we are able to artificially impose multiferroism in the epitaxially grown $TmFeO_3$ film below 120 K.

Multiferroic materials have attracted a great deal of interest over the past decade due to their fascinating physics of magnetoelectric couplings and their technological potential in data storages.[1-11] Among numerous multiferroics currently under investigation, manganites based multiferroics have been most extensively studied owing to their strong tendency of the magnetoelectric coupling. They are classified into two kinds of distinct crystal structures depending on the radius of rare-earth cation. $ReMnO_3$-type oxides with Re = La−Dy in the lanthanide series belong to orthorhombic manganites,[2,6,8] while $ReMnO_3$-type oxides with Re = Ho−Lu belong to hexagonal manganites.[12-14] Unlike orthomanganites, hexagonal manganites possess c-axis-oriented ferroelectricity owing to the disappearance of a mirror image on the a−b plane with a tilting of the MnO_5 bipyramid units.[12] They also exhibit an antiferromagnetic (AFM) order below the magnetic ordering temperature, as Mn^{3+} spins are oriented parallel to the a−b plane with a so-called 120° triangular spin structure.[13,15-17]

Contrary to the two distinct structural polymorphs observed in rare-earth manganites, all of the $ReFeO_3$-type oxides belong to orthorhombic ferrites (orthoferrites) and are characterized by corner-linked FeO_6 octahedra forming a three-dimensional network in a centrosymmetric Pnma (or Pbnm) unit cell.[18,19] Accordingly, all of the rare-earth orthoferrites are known to be non-ferroelectric at room temperature except for the recently reported improper ferroelectricity in $SmFeO_3$, which is caused by the canted AFM spin ordering through a reverse Dzyaloshinskii−Moriya interaction.[20] Considering the c-axis-oriented structural ferroelectricity observed in hexagonal manganites, we have been exploring the possibility of artificially imposing ferroelectricity and thus multiferroism by structurally tailoring an AFM orthoferrite, $ReFeO_3$, in a constrained thin-film form. Indeed, Bossak and co-workers[21] reported the fabrication of epitaxially stabilized hexagonal orthoferrite $ReFeO_3$ (Re = Eu−Lu) thin films on ZrO_2 (Y_2O_3) substrates. However, their study was limited to structural characterizations. Recently, we reported rare-earth ferrite heterostructures on sapphire (0001) substrates that have a six-fold hexagonal symmetry. Surprisingly, they all show the c-axis-oriented ferroelectricity up to their Curie temperatures. Among these artificial compounds, hexagonal $YbFeO_3$ reveals an interesting phenomenon of the characteristic two-step polarization decay associated with sequential phase transitions from $P6_3/mmc$ to $P6_3mc$ and $P6_3cm$.[22]

In this letter, we propose an artificially imposed multiferrosim in the $TmFeO_3$ thin film that is epitaxially constrained on a suitable hexagonal template. On the basis of our DFT (density functional theory) calculations, the asymmetric orbital hybridization between Tm $5d_z{}^2$ and O $2p_z$ is primarily responsible for the c-axis-oriented ferroelectricity. Interestingly, the observed ferroelectricity in hexagonal $TmFeO_3$ (h-TFO) shows a direct ferroelectric transition from the paraelectric $P6_3/mmc$ phase to the $P6_3cm$ ground state unlike the recently found h-$YbFeO_3$.

The hexagonal structure consists of FeO_5 bipyramid units having trigonal D_{3h} site symmetry and TmO_8 units with D_{3d} site symmetry, which involve with two different Tm sites, Tm1 and Tm2 (See Figure S2 in supplementary information). As shown in Fig 1(a), the TmO_8 units commonly share two kinds of oxygen ions with the FeO_5 units: i) two apical oxygen ions (O_A) along the c-axis and ii) six oxygen ions (O_I) in two triangular planes. Notice that these two units are separated to form a two-dimensional (2D) layered structure in contrast to 3D network structures of the FeO_6 octahedra corner-linked each other in perovskite.

As shown in Figure 1(b), the 2theta-theta X-ray diffraction pattern (XRD) indicates that the h-TFO film grown on a Pt(111)/Al_2O_3(0001) substrate by pulsed laser deposition method is highly c-axis oriented without any other phases. The in-plane heteroepitaxial relationship between h-TFO and the hexagonal template was further confirmed with phi(Φ)-scans measured at $(11\bar{2}2)$ for TFO and (200) for Pt [Fig 1(c)]. The scans exhibit the six-fold symmetry characteristic at the same azimuthal phi-angles for both h-TFO and Pt, presenting that the h-TFO film is epitaxially constrained on the hexagonal template.

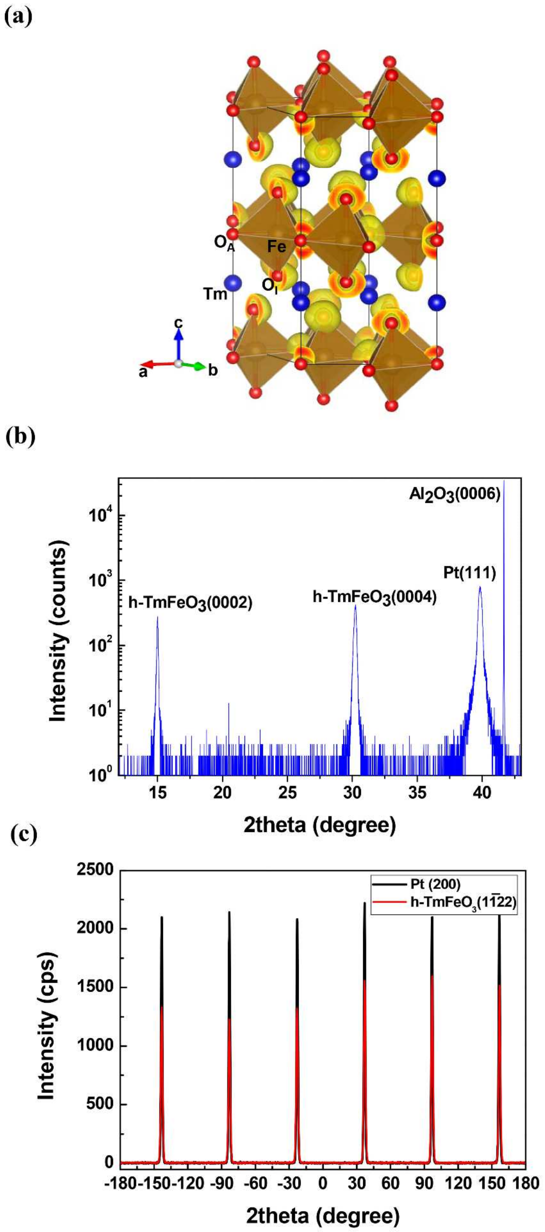

Fig. 1 (a) Unit-cell crystal structure of the hexagonal $TmFeO_3$ with the polar $P6_3cm$ state. (b) Theta-2theta X-ray diffraction (XRD) pattern of the preferential [0001]-oriented $TmFeO_3$ film prepared by pulsed laser deposition method. (c) The heteroepitaxial growth of h-TFO was confirmed by examining the in-plane XRD phi-scans. These patterns were obtained by keeping the Bragg angle at $(11\bar{2}2)$ for TFO and (200) for Pt.

We have measured polarization versus electric field (P-E) curves at 3 K and 300 K to examine the c-axis-oriented ferroelectricity in the heteroepitaxial h-TFO film. As shown in Figure 2(a), the h-TFO film shows saturated hysteresis loops at both temperatures. The ferroelectric characteristic was also confirmed by obtaining a butterfly-shaped hysteresis curve in the capacitance voltage measurement (See Figure S3 in supplementary information). The temperature-induced polarization was then determined by measuring a pyroelectric current and subsequently integrating the measured current as a function of the temperature. As shown in Figure 2(b), the spontaneous polarization begins to increase at ~430 K and reaches ~8.7 μC/cm^2 at 3K, which is comparable with remanant polarization values obtained from the P-E hysteresis loops. This indicates the onset of the para-to-ferroelectric transition. The temperature-dependent dielectric permittivity was further investigated to support this ferroelectric transition at ~430 K (See Figure S5 in supplementary information). It is interesting to notice that h-TFO exhibits a direct ferroelectric transition from the paraelectric state to the ground state without other intermediate phases in contrast to the recent report in the hexagonal $YbFeO_3$ compound. According to our first-principles calculations, the optimized crystal structure of h-TFO is the non-centrosymmetric $P6_3cm$ phase in the ground state, which is similar to YMO, the prototype of the h-$RMnO_3$ family. From these results, one can clearly conclude that h-TFO possess the c-axis-oriented ferroelectricity up to 430 K (T_C, Curie temperature) associated with the ferroelectric transition from the high temperature $P6_3/mmc$ phase to the ground $P6_3cm$ phase.

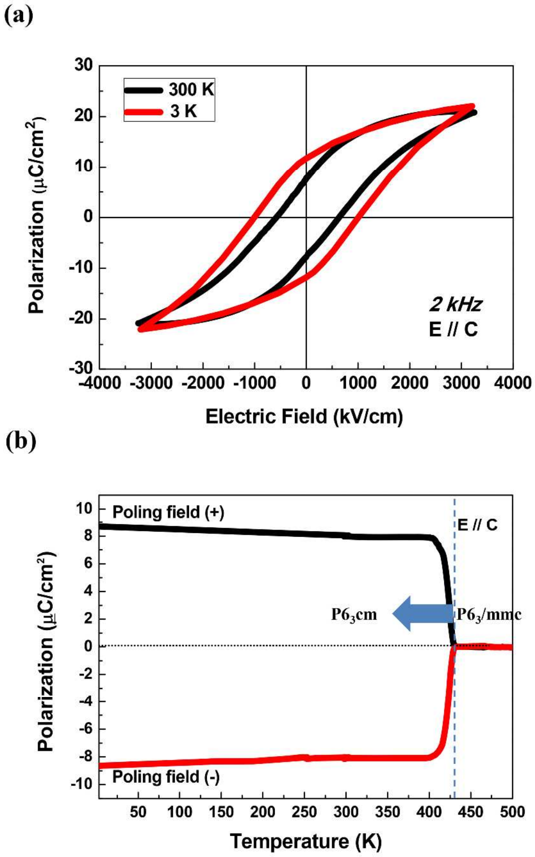

Fig. 2 (a) Polarization−field hysteresis loops obtained at 3 K and 300 K. (b) Temperature-dependent spontaneous polarization curve of the hexagonal $TmFeO_3$ thin film, showing a ferroelectric transition at 430 K

Having related with the ferroelectric origin, two conflicting mechanisms associated with a bonding nature are being debated. The two mechanisms are the ionicity or covalency between the rare earth ion and the oxygen ion. To clarify this issue, we first compare computed electron localization function (ELF) of the paraelectric $P6_3/mmc$ phase with that of the ferroelectric $P6_3cm$ phase on the basis of DFT calculations. In the centrosymmetric $P6_3/mmc$ phase, as shown in Figure 3(a), the ELF between the Tm ion and the axial oxygen (O_A) is relatively negligible suggesting that the ionic bond is mainly involved in the Tm-O_A bond. However, the Tm ion moves to an asymmetric position and there occurs an orbital mixing between the Tm ion and one of the two O_A ions along the c-axis upon the ferroelectric transition to the $P6_3cm$ phase (Red and blue arrows indicate the direction of the atomic movement upon the ferroelectric transition). This indicates that the asymmetric covalent bond along the c-axis is predominantly responsible for the ferroelectricity in the $P6_3cm$ phase.

To puzzle out what kinds of orbital interactions are involved in the covalent bonding, we have further examined partial density of states (PDOS) for various bonding orbitals. According to our careful analysis of PDOS as shown in Figure 3(b), it shows a strong overlapping between the Tm $5d_{z^2}$-orbital and the apical O_A $2p_z$-orbital in the $P6_3cm$ phase, while there is no significant hybridization in the $P6_3/mmc$ phase. Thus, one can conclude that the covalent bond associated with the hybridization between Tm $5d_z{}^2$ and O $2p_z$ orbitals is the electronic origin in the hexagonal h-TFO compound.

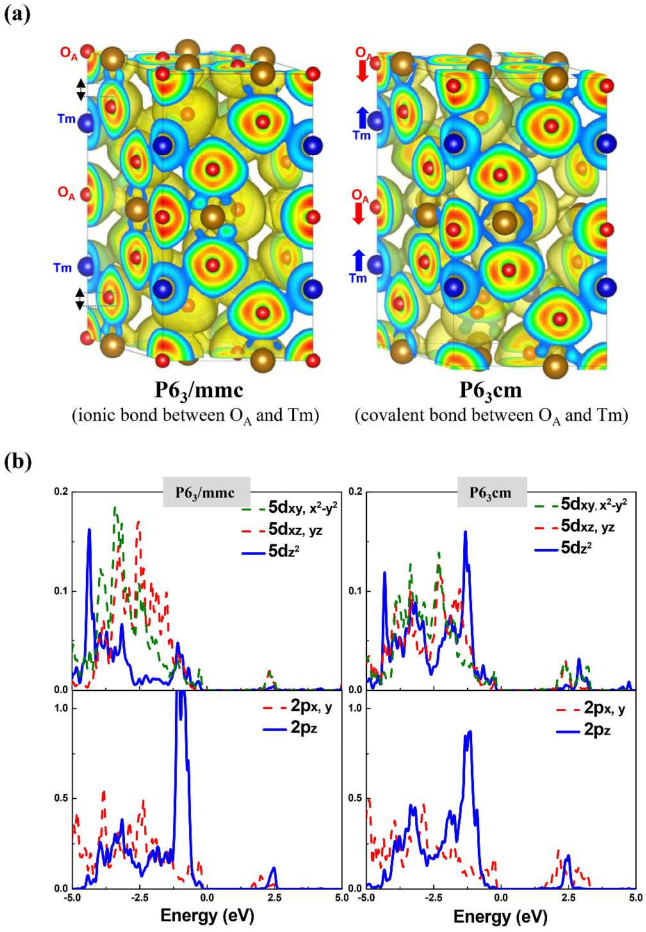

Fig. 3(a) Three-dimensional electron-density contour of the paraelectric $P6_3/mmc$ phase is compared with that of the $P6_3cm$ ferroelectric phase. (b) Comparison of the orbital-resolved partial density of states for $5d_z{}^2$(Tm), and $2p_z(O_A)$ orbitals of the paraelectric $P6_3/mmc$ phase with that of the ferroelectric $P6_3cm$ phase.

Let us now examine a magnetic spin ordering in the h-TFO thin film. For this purpose, we measured the temperature-dependent magnetization under both zero-field-cooled (ZFC) and field-cooled (FC) conditions. As shown in Figure 4(a), the ZFC and FC curves along the c-axis indicate a Neel temperature (T_N) at ~120 K, suggesting the onset of long-range magnetic ordering. In the magnetization-field hysteresis curves under various temperatures [Figure 4(b)], we observe that magnetic spins begin to respond the external magnetic field below ~150 K, and the magnetic remanence (M_R) increases with decreasing temperature. Hence, we can infer from the above results that h-TFO exhibits long-range magnetic ordering below T_N, ~120 K.

It is well known that the magnetic spins of Fe^{3+} are oriented parallel to the ab-plane with a so-called 120° structure in hexagonal rare-earth ferrites.[13-16] This configuration is a typical spin structure for triangular antiferromagnetic (AFM) lattice in frustrated magnetic systems such as hexagonal manganites. Thus, a nearly zero residual moment is expected along the in-plane direction. The Fe^{3+} spins, however, are slightly canted with a non-zero magnetic net moment along the c-axis in contrast to the zero residual moment along the in-plane. The onset of the magnetic ordering below ~120 K as observed in the temperature-dependent magnetization curve is associated with the canted net moment of Fe^{3+} spins along the c-axis.

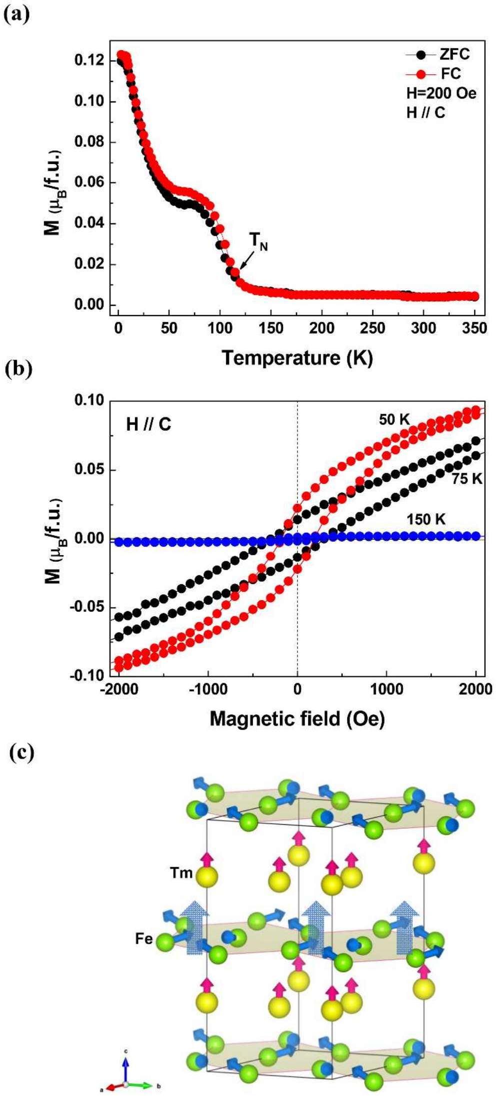

Fig. 4 (a) Temperature-dependent magnetization curves (ZFC and FC) showing the onset of the long-range magnetic ordering below ~120 N. (b) Magnetization−field hysteresis curves obtained at various temperatures. (c) Proposed ground-state spin configuration in hexagonal $TmFeO_3$. The spins at the Tm^{3+} ion sublattice are marked with red arrows, whereas the spins at the Fe^{3+} ion sublattice are denoted by blue arrows.

In addition to the antiferromagnetic interaction of Fe^{3+} ions below ~120 K, other types of magnetic interactions between Tm^{3+} and Tm^{3+} or Tm^{3+} and Fe^{3+} are expected in h-TFO as the sample is further cooled down to 3 K. According to recent results by Fiebig's group,[23,24] magnetic spins in these hexagonal multiferroics could be reoriented due to magnetic superexchange interactions between the two different magnetic ions (Tm^{3+} and Fe^{3+}). In our h-TFO thin film, therefore, the magnetic phase transition observed at ~70 K seems to have a close relation to the superexchange interactions between them. This phenomenon is currently under investigations.

According to our previous results based on DFT calculations, the magnetic spins of rare-earth ions tend to be aligned ferromagnetically at the ground state. In addition, the spin direction of the rare-earth ions (-c) is opposite to that of the canted Fe^{3+}-spin moment (+c).[20,22,25] The DFT calculations further predicted that the magnitude of the orbital and spin moment of the rare-earth ions is much bigger than that of the canted Fe^{3+}-spin moment, leading to the magnetization reversal below T* (compensation temperature).[22] In the case of h-TFO, however, the ZFC curve follows the FC curve without the magnetization reversal as temperature decreases. This result suggests that the magnetic spins of Tm^{3+} ions are aligned ferromagnetically along the same direction as the canted Fe^{3+}-spin moment. The proposed spin configuration in h-TFO is illustrated in Figure 4(c).

Conclusions

In summary, we have shown that h-TFO exhibits multiferroism, i.e. simultaneously ferroelectricity and ferromagnetism below 120 K. The h-TFO thin film is ferroelectric up to ~430 K, and the ferroelectricity is characterized as the direct ferroelectric transition from the high temperature $P6_3/mmc$ phase to the ground $P6_3cm$ phase without other intermediate phases. According to our DFT calculations, the c-axis-oriented orbital hybridization between Tm^{3+} $5d_{z^2}$ and O^{2-} $2p_z$ is mainly responsible for the observed ferroelectricity. In addition, we suggest that the ferromagnetic behavior is attributed to the long-range spin ordering of Tm^{3+} ions along the same direction as the canted Fe^{3+} spin moment.

Notes and references

[a] Department of Materials Science and Engineering, and Division of Advanced Materials Science, Pohang University of Science and Technology (POSTECH), Pohang 790-784, Republic of Korea.

[b] Department of Materials Science and Engineering, Northwestern University, Evanston, IL 60208 USA.

[c] Memory Manufacturing Operation Center, Samsung Electronics Co., Ltd., Hwaseong-si, 449-711, Republic of Korea.

† Electronic Supplementary Information (ESI) available: [Kohn-sham (K-S) energy as a function of the off-center displacement of the Tm ion, local distances between Tm and O ions, optimized atomic positions, capacitance-voltage curve, pyroelectric current curve, temperature-dependent dielectric permittivity curve].
See DOI: 10.1039/c000000x/

1 J. Wang, J. B. Neaton, H. Zheng, V. Nagarajan, S. B. Ogale, B. Liu, D. Viehland, V. Vaithyanathan, D. G. Schlom, U. V. Waghmare, N. A. Spaldin, K. M. Rabe, M. Wuttig, and R. Ramesh, *Science*, 2003, **299**, 1719.
2 T. Kimura, T. Goto, H. Shintani, K. Ishizaka, T. Arima, and Y. Tokura, *Nature*, 2003, **426**, 55.
3 N. Hur, S. Park, P. A. Sharma, J. S. Ahn, S. Guha, and S. W. Cheong, *Nature*, 2004, **429**, 392.
4. T. Lottermoser, T. Lonkai, U. Amann, D. Hohlwein, J. Ihringer, M. Fiebig, *Nature*, 2004, **430**, 541.
5 N. A. Spaldin and M. Fiebig, *Science*, 2005, **309**, 391.
6 H. Katsura, N. Nagaosa, A.V. Balatsky, *Phys. Rev. Lett*., 2005, **95**, 057205
7 W. Eerenstein, N. D. Mathur, J. F. Scott, *Nature*, 2006, **442**, 759.
8 A. A. Belik, T. Furubayashi, Y. Matsushita, M. Tanaka, S. Hishita, E. Takayama-Muromachi, *Angew., Chem. Int. Ed*., 2009, **48**, 6117.
9 S.-W. Cheong, M. Mostovoy, *Nature Mater.,* 2007, **6**, 13.
10 Y. Tokunaga, N. Furukawa, H. Sakai, Y. Taguchi, T. Arima, Y. Tokura, *Nature Mater.,* 2009, **8**, 558.
11 T. Choi, Y. Horibe, H. T. Yi, Y.J Choi, W. Wu, S.-W. Cheong, *Nature Mater*., 2010, **9**, 253.
12 B. B. Van Aken, T. T. M. Palstra, A. Filippetti, N. A. Spaldin, *Nature Mater.*, 2004, **3**, 164.
13 H. Lueken, *Angew. Chem., Int. Ed*., 2008, **47**, 8562.
14 C.-Y. Ren, *Phys. Rev. B,* 2009, **79**, 125113.
15 M.-A. Oak, J.-H. Lee, H. M. Jang, J. S. Goh, H. J. Choi, J. F. Scott, *Phys. Rev. Lett*., 2011, **106**, 047601.
16 T. Katsufuji, M. Masaki, A. Machida, M. Moritomo, K. Kato, E. Nishibori, M. Takata, M. Sakata, K. Ohoyama, K. Kitazawa, H. Takagi, *Phys. Rev. B*, 2002, **66**, 134434.
17 X. Fabrèges, S. Petit, I. Mirebeau, S. Pailhès, L. Pinsard, A. Forget, M. T. Fernandez-Diaz, F. Porcher, *Phys. Rev. Lett*., 2009, **103**, 06720.
18 R. L. White, *J. Appl. Phys*., 1969, **40**, 1061.
19 M. Marezio, J. P. Remeika, P. D. Dernier, *Acta Crystallogr. B,* 1969, **26**, 2008
20 J.-H. Lee, Y. K. Jeong, J. H. Park, M.-A. Oak, H. M. Jang, J. Y. Son, J. F. Scott, *Phys. Rev. Lett.,* 2011, **107**, 117201.
21 A. A. Bossak, I. E. Graboy, O. Y. Gorbenko, A. R. Kaul, M. S. Kartavtseva, V. L. Svetchnikov, H. W. Zandbergen, *Chem. Mater*., 2004, **16**, 1751.
22 Y. K. Jeong, J.-H. Lee, S.-J. Ahn, S.-W. Song, H. M. Jang, H. Choi, J. F. Scott, *J. Am. Chem. Soc*., 2012, **134**, 1450.
23 M. Fiebig, C. Degenhardt, R. V. Pisarev, *Phys. Rev. Lett.*, 2002, **88**, 027203.
24 P. Murugavel, J.-H. Lee, D. Lee, T. W. Noh, Younghun Jo, Myung-Hwa Jung, Yoon Seok Oh, Kee Hoon Kim, *Appl. Phys. Lett*., 2007, **90**, 142902.
25 Y. K. Jeong, J.-H. Lee, S.-J. Ahn, H. M. Jang, *Solid state commun*., 2012, **152**, 1112.

Journal Name

RSCPublishing

COMMUNICATION

A Table of Contents

The hexagonal $TmFeO_3$ film shows a ferroelectric transition from the paraelectric *$P6_3/mmc$* phase to the *$P6_3cm$* ground state at ~430 K by the c-axis-oriented orbital hybridization between Tm and O ions.